The Potential Impact of Regional Climate Change on Fire Weather in the United States

Ying Tang,* Shiyuan Zhong,* Lifeng Luo,* Xindi Bian,† Warren E. Heilman,† and Julie Winkler*

*Department of Geography, Michigan State University
†U.S. Department of Agriculture Forest Service

Climate change is expected to alter the frequency and severity of atmospheric conditions conducive for wildfires. In this study, we assess potential changes in fire weather conditions for the contiguous United States using the Haines Index (HI), a fire weather index that has been employed operationally to detect atmospheric conditions favorable for large and erratic fire behavior. The index summarizes lower atmosphere stability and dryness into an integer value with higher values indicting more fire-prone conditions. We use simulations produced by the North American Regional Climate Change Assessment Program (NARCCAP) from multiple regional climate models (RCMs) driven by multiple general circulation models (GCMs) to examine changes by midcentury in the seasonal percentage of days and the consecutive number of days with high (values $\geq$ 5) HI across the United States. Despite differences among the six RCM–GCM combinations in the magnitude and location of the projected changes, the results consistently suggest an increase in the number of days with high HI values over most of the United States during the summer season, with the dryness factor of the HI contributing more than the stability parameter to the projected changes. In addition, the consecutive number of days with high HI is projected to increase in summer. Together, these results suggest that future summers might be more conducive to large and dangerous fires. The projections for other seasons are inconsistent among the model combinations. *Key Words: climate change, Haines Index, NARCCAP, wildfire.*

气候变迁被认为会改变导致森林大火的大气条件之频率与剧烈程度。我们在此研究中，运用海恩斯指数（HI）——一个操作上用来侦测对大型且不规律的火灾行为有利的气候条件的火灾气侯指数，评估美国大陆上火灾气候条件的可能改变。该指数将较低的大气稳定度与乾燥程度概括进一个整体数值，而较高的数值则指向更易导致火灾的条件。我们运用北美区域气候变迁评估计画（NARCCAP）从由多种大气环流模式（GCMs）所驱动的多重区域气候模式（RCMs）中所生产的模拟，检视美国到世纪中期时，具有高度HI（数值大于五）的每季日数比例和连续日数的改变。儘管六个RCM-GCM的结合，在预期改变的幅度与地点上虽有所差异，但研究结果一致指出，美国多处地方于夏季时，具有高度HI数值的日数将有所增加，而HI的乾燥因素，将较稳定性的因素，对预测的改变产生更大影响。此外，连续具有高度HI的日数，预期将在夏季有所增加。这些研究结果共同显示，未来的夏季可能会更倾向引发大型且危险的火灾。其他季节的预测，则在模式组合中不尽一致。*关键词：气候变迁，海恩斯指数，北美区域气候变迁评估计画 (NARCCAP)，森林大火。*

Es de esperarse que el cambio climático altere la frecuencia y severidad de las condiciones atmosféricas que puedan propiciar incendios naturales. En este estudio sopesamos los cambios potenciales de las condiciones del tiempo con estas características en los Estados Unidos contiguos mediante el Índice Haines (HI), un índice del tiempo propiciador del fuego que ha sido empleado operacionalmente para detectar condiciones favorables a la aparición de escenarios para fuegos erráticos y del alta intensidad . El índice compendia las condiciones de estabilidad y sequedad de la atmósfera inferior en un valor integral en el que los valores más altos acusan condiciones de una mayor propensión al incendio. Utilizamos las simulaciones desarrolladas en el Programa Norteamericano de Evaluación Regional del Cambio Climático (NARCCAP) a partir de múltiples modelos regionales de clima (RCMs) condicionados por múltiples modelos de circulación general (GCMs) para examinar los cambios de mediados de siglo en el porcentaje estacional de días y el número consecutivo de días con altos valores HI (valores_5) a través de los Estados Unidos. Pese a diferencias entre las seis combinaciones RCM–GCM por magnitud y localización de los cambios proyectados, los resultados son consistentes para sugerir un incremento durante el verano en el número de días con valores HI altos en la mayor parte de los Estados Unidos, cuando el factor de sequedad del HI contribuye más que el parámetro de estabilidad de los cambios proyectados. Adicionalmente, se proyecta que el número consecutivo de días con HI alto se incremente en el verano. En conjunto, estos resultados sugieren que en el futuro los veranos podrían ser más propensos a incendio grandes y peligrosos. Las proyecciones para otras estaciones son inconsistentes dentro de las combinaciones del modelo. *Palabras clave: cambio climático, Índice de Haines, NARCCAP, incendios naturales.*

Annals of the Association of American Geographers, 105(1) 2015, pp. 1–21
Initial submission, February 2014; revised submission, July 2014; final acceptance, August 2014
Published by Taylor & Francis, LLC.

Wildfires pose significant threats to life and property in many regions of the United States. Wildfire incidents are largely driven by natural factors including fuel availability, temperature, precipitation, wind, humidity, and the location of lightning strikes, although anthropogenic factors such as land use and fuel management practice also contribute to wildfire occurrences (Westerling et al. 2003). Long-term climate change will likely affect these natural factors, with implications for future wildfire danger. Various indexes have been developed to help assess the potential for wildfires. The assumption behind these indexes is that the constant and variable factors that affect the initiation, spread, and difficulty of control of wildfires can be summarized into simple numerical descriptors (Deeming, Burgan, and Cohen 1977). Widely used indexes include the Keetch–Byram Drought Index (KBDI), an estimate of forest fire potential based on the daily water balance (Keetch and Byram 1968); the Burning Index (BI), a description of the effort needed to contain a fire (Bradshaw et al. 1984); the Energy Release Component (ERC), an estimate of the twenty-four-hour total available energy per unit area within the flaming front at the head of a fire (Bradshaw et al. 1984); the thousand-hour fuel moisture (THFM), a representation of the modeled moisture content in dead fuels (Bradshaw et al. 1984); and the Haines Index (HI), a measure of how conducive the atmosphere is to potential extreme or erratic fire behavior based on atmospheric stability and moisture (Haines 1988).

Fire weather indexes are often used locally or regionally to assist in decision making, and considerable research has been conducted on the relationship between fire weather indexes and actual fire occurrences (Dayananda 1977; Mandallaz and Ye 1997; Preisler et al. 2004; Preisler and Westerling 2007). Also, as the values of these indexes can vary substantially at regional and continental scales (Werth and Werth 1998; Winkler et al. 2007; Lu et al. 2011), a number of studies have used fire weather indexes to study wildland fire danger across the continental United States under projected future climate conditions. For example, Brown, Hall, and Westerling (2004) employed the ERC to investigate the potential impact of twenty-first-century climate change on the number of days with high fire danger in the Western United States using high-temporal resolution meteorological output from the parallel climate model. Liu, Stanturf, and Goodrick (2010) applied the KDBI to simulations from several general circulation models (GCMs) to estimate future changes in fire season length for the United States.

This study examines potential changes in the atmospheric conditions favoring extreme fire behavior as indicated by differences in the HI between the current and projected future climate. Extreme fire behavior is defined by the National Oceanic and Atmospheric Administration (2014) as "a level of wildfire behavior that ordinarily precludes methods of direct attack" and "predictability is difficult because such fires often exercise some degree of influence on their environment, behaving erratically, sometimes dangerously." This focus on extreme fire behavior reflects concerns that wildfires recently have become more extreme. Although the number of wildfires in the United States has been relatively stable since 1984 (National Interagency Fire Center 2013), the total area burned has increased, particularly in recent years and despite interannual fluctuations related to natural climate variability (Figure 1), suggesting larger and more extreme wildfires. Given that more erratic fire behavior could lead to increased area burned (Parisien et al. 2005), projecting future changes in extreme or erratic fire behavior would be very helpful for fire management. Furthermore, large and megafires are responsible for 80 percent of fire suppression costs in the United States (Williams 2004).

The HI, originally introduced in 1988 as the Lower Atmospheric Severity Index, is widely used to assess the potential for a plume-dominated fire to become large or exhibit extreme fire behavior (Haines 1988; Winkler et al. 2007; Lu et al. 2011). The HI is used operationally in wildfire forecasting and monitoring and is a standard element in the National Weather Service daily fire weather forecasts and the U.S. Department of Agriculture Forest Service's Wildland Fire Assessment System. Considered primarily a regional index, the HI can provide a perspective on fire risk over large areas (Heilman and Bian 2007).

Another motivation for using the HI to study future wildfire risk is that several historical climatologies of this index are available for the United States and provide a useful reference for evaluating future changes. The first comprehensive long-term and spatially extensive climatology of the HI was produced by Winkler et al. (2007), who employed temperature and dewpoint data from the National Centers for Environmental Prediction (NCEP) global reanalysis for a forty-year (1961–2000) period on a 2.5° by 2.5°

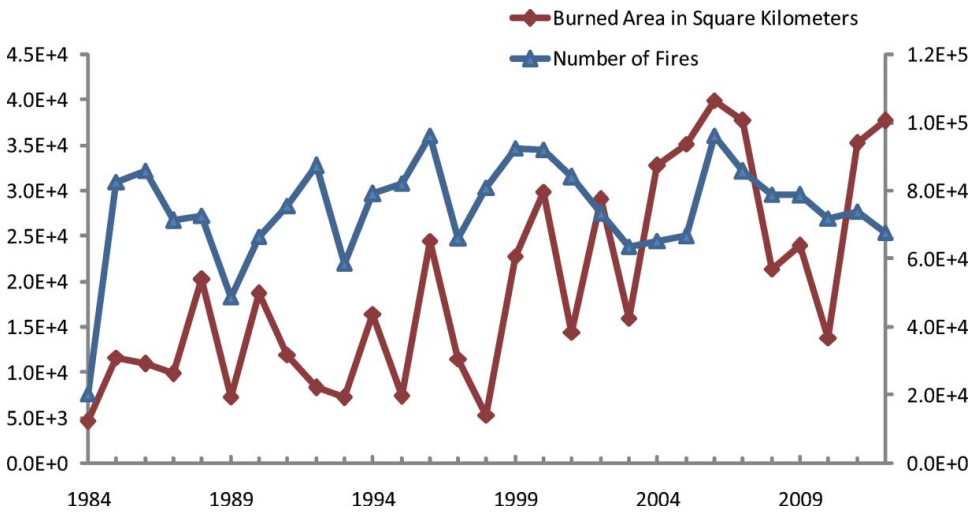

Figure 1. Burned area (left axis) and number of wildland fires (right axis) in the United States from 1984 to 2012. The National Interagency Coordination Center at the National Interagency Fire Center compiles annual wildland fire statistics for federal and state agencies. 2004 fires and acres do not include state lands for North Carolina. (Color figure available online.)

latitude and longitude grid for the North American domain. Before that, climatological analyses were generally confined temporally and geographically (Jones and Maxwell 1998; Werth and Werth 1998; Croft, Watts, and Potter 2001). More recently, Lu et al. (2011) improved on the spatial resolution of the Winkler et al. (2007) climatology using 32 km resolution temperature and dewpoint fields from the North American Regional Reanalysis (NARR). In spite of the large differences in resolution, the spatial distributions of the HI for the two climatologies are similar for most of North America, with generally higher HI values in the west than in the east. The largest differences between the two climatologies are found along coastlines and in areas of complex terrain.

A number of previous studies have employed simulations from GCMs and regional climate models (RCMs) to assess the impact of climate change on fire activity. For example, Golding and Betts (2008), using the McArthur Forest Fire Danger Index and an ensemble of variants of the Hadley Centre Coupled Model version 3 (HadCM3; Gordon et al. 2000) climate model, found a significant increase over the twenty-first century in fire risk for Amazonia due to climate change and deforestation. Similarly, the risk of forest and grassland fires in Australia is anticipated to increase by 2050 and 2100 based on simulations from the Regional Atmospheric Modeling System (RAMS; Pielke et al. 1992; Pitman, Narisma, and McAneney 2007). Spracklen et al. (2009) applied a regression model built based on observed area burned and observed climate to the output from the Goddard Institute for Space Studies (GISS; Schmidt et al. 2006) GCM and estimated that increases in temperature will cause substantial increases by 2050 in the annual mean area burned in the Western United States. In addition, HI values estimated from a suite of RCM simulations suggest that atmospheric environments in the mountainous regions of the Western United States during August will be more conducive to erratic wildfires by the middle of the twenty-first century (Luo et al. 2013). A review of additional studies that used GCMs or RCMs to investigate global wildland fire activity under climate change can be found in Flannigan et al. (2009).

The objective of our study is to investigate how atmospheric conditions conducive to extreme fire behavior will change in a changing climate. Most of the previous studies of climate impacts on fire weather conditions have used climate projections from either a single high-resolution RCM (Liu, Goodrick, and Stanturf 2013) with no estimates of uncertainties or multiple coarse-resolution GCMs (Flannigan, Stokes, and Wotton 2000; Flannigan et al. 2005) with poor resolution of heterogeneity in terrain and land cover. This study attempts to overcome these limitations by examining changes in the HI between current and future climates, based on climate projections from multiple RCMs driven by multiple GCMs. Winkler et al. (2011) pointed out that no single RCM performs best all the time; the performance depends on the field examined, and the uncertainty introduced by the choice of RCMs can be as large as the choice of GCMs. By comparing results from various combinations of GCMs and RCMs, it is possible to evaluate the robustness of the model results regarding potential

changes in atmospheric conditions conducive to large and extreme wildland fires. Thus, the results will provide not only information on the potential changes but also the associated uncertainties, a key factor to consider in the decision-making process. The analysis focuses on the time of the year and the regions within the United States most likely to be affected by climate change. These findings will help fire and resource managers in designing climate change adaptation strategies.

Data and Methods

Data

The data sets used to generate the HI climatology were provided by the North American Regional Climate Change Assessment Program (NARCCAP; Mearns et al. 2007; Mearns et al. 2009). Aimed at producing high-resolution climate-change simulations for use in assessment studies, the NARCCAP program performed climate simulations using a suite of RCMs driven by a set of GCMs for North America (Mearns et al. 2007; Mearns et al. 2009; Mearns et al. 2012). A 50-km horizontal grid spacing was used for all of the RCM simulations. Simulations were produced for both the current climate period from 1971 to 2000 (henceforth referred to as GCM-driven current climate) and a future climate period from 2041 to 2070 (henceforth referred to as GCM-driven future climate). For the twenty-first century, the GCMs were forced with the A2 emissions scenario, which describes a very heterogeneous world with continuously increasing global population and regionally oriented economic growth (Nakicenovic et al. 2000). In addition to the GCM-driven current climate simulations, another set of RCM simulations driven by the NCEP global reanalysis for the period from 1979 to 2004 (henceforth referred to as NCEP-driven current climate) was also produced by NARCCAP to evaluate the RCM simulations. According to Giorgi (2006), reanalysis products such as the NCEP global reanalysis, which are created by assimilating weather and climate observations using models, can be expected to provide the best available large-scale forcing fields for regional simulations. Regional simulations driven by reanalysis data at lateral boundaries are often referred to as *perfect boundary condition simulations*. Thus, the NCEP-driven current climate can be compared to observed climate series or fields to identify systematic model errors (Winkler et al. 2011). The GCM-driven current climate simulation is often referred to as the control run, and differences between GCM-driven current climate and NCEP-driven current climate simulations are assumed to be introduced by the GCM fields. To assess future changes, the GCM-driven current climate is compared with GCM-driven future climate, as it contains errors from both the GCM and RCM, whereas the NCEP-driven current climate only contains the RCM errors (Winkler et al. 2011).

Table 1. North American Regional Climate Change Assessment Program model combination outputs used in this study

	GCM-driven			NCEP-driven
RCM	GFDL	CGCM3	CCSM	NCEP
RCM3	X	X		X
CRCM		X	X	X
WRFG		X	X	X

Note: GCM = general circulation model; NCEP = National Centers for Environmental Prediction; RCM = regional climate model; GFDL = Geophysical Fluid Dynamics Laboratory GCM; CGCM3 = Canadian Global Climate Model version 3; CCSM = Community Climate System Model; RCM3 = Regional Climate Model version 3; CRCM = Canadian Regional Climate Model; WRFG = Weather Research and Forecasting Grell model.

The set of RCMs used in this study includes the Canadian Regional Climate Model (CRCM; Laprise et al. 1998; Caya and Laprise 1999), the Weather Research and Forecasting Grell model (WRFG; Grell and Devenyi 2002; Skamarock et al. 2005), and the Regional Climate Model version 3 (RCM3; Pal et al. 2007). The driving GCMs include the NCAR Community Climate System Model (CCSM; Collins et al. 2006), the Canadian Climate Centre's Canadian Global Climate Model version 3 (CGCM3; Flato 2005), and the Geophysical Fluid Dynamics Laboratory GCM (GFDL; Delworth et al. 2006). The NARCCAP model combinations are shown in Table 1. Simulations from six RCM–GCM combinations and three RCM–NCEP combinations are analyzed. For details on the mode configurations and physics parameterizations used for these simulations, please refer to http://www.narccap.ucar.edu/about/index.html.

Haines Index Calculation

The HI consists of an atmospheric stability component (A) and a humidity component (B; Haines

Table 2. Calculation of the Haines Index A and B components for the three elevation variants

	Stability component (A)		Humidity component (B)	
Elevation	Calculation	Categories	Calculation	Categories
Low	950 hPa temperature – 850 hPa temperature	A = 1 if < 4 A = 2 if 4–7 A = 3 if ≥ 8	850 hPa temperature – 850 hPa dewpoint	B = 1 if < 6 B = 2 if 6–9 B = 3 if ≥ 10
Mid	850 hPa temperature – 700 hPa temperature	A = 1 if < 6 A = 2 if 6–10 A = 3 if ≥ 11	850 hPa temperature – 850 hPa dewpoint	B = 1 if < 6 B = 2 if 6–12 B = 3 if ≥ 13
High	700 hPa temperature – 500 hPa temperature	A = 1 if < 18 A = 2 if 18–21 A = 3 if ≥ 22	700 hPa temperature – 700 hPa dewpoint	B = 1 if < 15 B = 2 if 15–20 B = 3 if ≥ 21

Note: Temperature and dewpoint are in Celsius.

1988). The A component is calculated as the temperature difference between two pressure levels (i.e., the lapse rate or the rate at which temperature decreases with altitude) in the lower atmosphere, and the B component represents the difference between temperature and dewpoint (i.e., the dewpoint depression) for a specific pressure level in the lower atmosphere. Each component is converted to an integer value of 1, 2, or 3 based on the prescribed thresholds shown in Table 2. The A and B components are summed to yield an HI value ranging from 2 to 6, with 2 representing a very low potential for erratic plume-dominated fires and 6 representing a very high potential (Haines 1988).

The temperature and humidity data for calculating the HI originally came from radiosonde observations. Although routine radiosonde observations are available two times per day at 0000 and 1200 UTC, the original HI was calculated using only the 0000 UTC soundings because this time is closer to the time of the day in most of North America when the instability is high and relative humidity is low, posing greater fire danger. Several studies have discussed the potential bias of using observations at other times and agreed that HI values based on 1200 UTC observations might underestimate fire potential because this is the time in North America when normally the atmosphere is stable (Jones and Maxwell 1998; Kochtubajda et al. 2001). Thus, only 0000 UTC data from NARR are used in this study, despite the availability of the NARR data at eight times per day.

In the initial index development, the United States was divided into three regions (referred to as low, mid, and high) to take into account variations in surface elevation. Three different variants of the HI were formulated so that the pressure layer used in the index calculation is "high enough above the surface to avoid the major diurnal variability of surface temperature and surface-based inversions" (Haines 1988, 23). Winkler et al. (2007) reproduced the boundaries for the three variants by comparing Haines's original map to elevation contours and found that the 300 m and 1,000 m contours best outline the original boundaries between the low variant and the mid variant and between the mid variant and the high variant respectively. In this study, the boundaries between the low, mid, and high variants are outlined, after Winkler et al. (2007), by contouring the 300 m and 1,000 m elevations of the topography used for each RCM simulation.

Wildfire danger is examined for the entire year rather than for a single month (Luo et al. 2013) or only the warm season (Lu et al. 2011), as the seasonality of wildfires varies spatially. As shown by Westerling et al. (2003), wildfires in the Western United States are strongly seasonal, with 94 percent of fires and 98 percent of area burned occurring between May and October and peak fire activity occurring during July and August. In the eastern United States, fire activity is more frequent in spring and fall (Knapp, Estes, and Skinner 2009). Whereas most states have a particular time of the year for wildfires, wildfire season in Florida is year-round.

For the GCM-driven current, GCM-driven future, and NCEP-driven current climates, the spatial distributions of the probability of the HI equal to or exceeding a given category (i.e., HI ≥ 2, 3, 4, 5, 6) are examined for each of the RCM–GCM or RCM–NCEP combinations. The probability for a specific

month is simply the number of days in that month when HI values equaled or exceeded a certain category, averaged over all years in the simulation period divided by the total number of days in the month. Calculations were performed for each month of the year but, to simplify the discussion, only the results from March, August, and October, representing the spring, summer, and autumn seasons, respectively, are presented. Although there are some variations within each season, the differences are much smaller compared to the interseasonal variability. Changes in the distribution of high (HI $\geq$ 5 or HI = 6) HI values, indicating a greater potential for large and erratic fires, are highlighted. Additionally, the percentage of days with high values of the stability component (A = 3) and the moisture component (B = 3) are examined separately to evaluate their relative contributions to changes in the HI.

Changes in the persistence of high ($\geq$ 5) HI values are also considered, as long periods of consistently high HI values are of special concern for fire managers. Persistence is quantified by the number of consecutive days with high HI values. The average length of all events as well as events longer than a certain number of days are computed and the changes in the average length of high HI events are examined.

As not all of the model combinations are in the same projection and grid setting, the HI values and probabilities for each model combination were resampled and reprojected from curvilinear grids to a common rectilinear grid based on the grid setting of the CRCM-ccsm simulations for further analysis. The weighting method used in the interpolation is the simple inverse distance squared scheme, where nearby values exert more influence on the interpolated value. The mean and standard deviation of the HI probabilities were calculated for each grid point on the standard grid. The standard deviation measures the spread of the model projections and helps to assess the consistency or the robustness of the results among model combinations. Even though the sample size is small, the resulting standard deviation maps provide an indication of where the different model combinations have the most similar or dissimilar values. It is important to bear in mind, though, that model consensus should not be confused with skill or reliability, as the RCM–GCM combinations share similar numerical schemes and parameterizations and thus are not independent (Winkler, Arritt, and Pryor 2014).

Results

As an HI value of 5 or 6 indicates a higher potential of erratic fire behavior, only results for HI $\geq$ 5 are presented here, even though HI values for all possible categories were calculated. Similarly, we focus on the highest category of the A and B components in the following discussion.

Percentage of Days with HI $\geq$ 5

GCM-Induced Biases in Current Climate Simulations

As discussed earlier, RCM simulations driven by GCMs contain errors generated not only by the RCMs but also from the GCMs through boundary conditions. On the other hand, RCM simulations driven by NCEP reanalysis data, which are often referred to as the perfect boundary condition (Giorgi 2006), are assumed to contain errors only from the RCMs. Thus, a comparison of GCM-driven current climate simulations with NCEP-driven current climate allows for an identification of errors introduced by the GCMs. Figure 2 shows the difference in the percentage of days with HI $\geq$ 5 between the GCM-driven and NCEP-driven current climate simulations. Red shading is associated with positive GCM biases (larger simulated percentages for the GCM-driven compared to NCEP-driven model runs) and blue shading is associated with negative GCM biases (GCM-driven simulation percentages less than the NCEP-driven values).

Over most of the United States, GCM-induced biases are greater during summer, in contrast to spring and fall, when biases are generally within $\pm$15 percent. Simulation results obtained with the same RCM but different GCMs show more similarity than those obtained with the same GCM but different RCMs.

Positive biases are observed across most of the United States with the CRCM-ccsm and CRCM-cgcm3 simulations in August, with the largest biases occurring in the Intermountain West and the Southeast. The CRCM-cgcm3 simulation yielded negative biases in the northern Plains and along the Texas coast. The WRFG-ccsm and WRFG-cgcm3 simulations also produced positive biases in the Intermountain West and negative biases in southern Texas, the Pacific Northwest, and parts of the northern Plains. In contrast, the RCM3-gfdl and RCM3-cgcm3 simulations produced negative biases in the northern half of the United States, especially in the northern Plains.

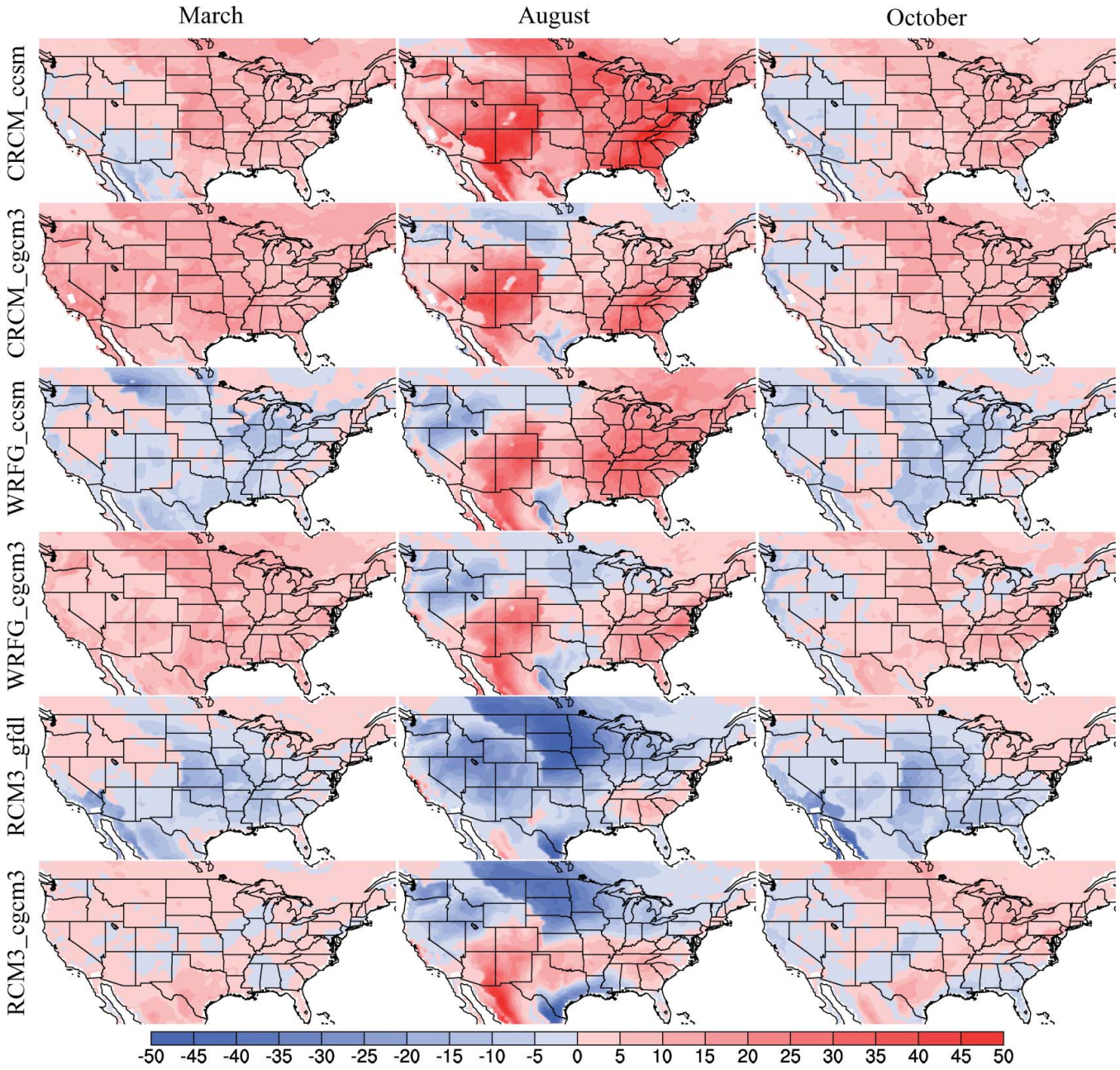

Figure 2. Differences in percentage of days for HI ≥ 5 in the United States for six model combinations between current and National Centers for Environmental Prediction climate for March (left column), August (center column), and October (right column). (Color figure available online.)

Negative biases covered most of the United States, with the exception of portions of the Southeast, for the RCM3-gfdl simulation, whereas for the RMC3-cgcm3 simulation, negative biases occurred in the northern half of the United States with positive biases over much of the southern half except for southern Texas, Louisiana, and Mississippi. In summary, there is considerable spatial variation in the GCM-induced biases for the different model combinations and across seasons.

Spatial and Seasonal Variations in Frequency for the GCM-Driven Current Climate

In general, the overall spatial and seasonal patterns are similar, especially those of the two WRFG

simulations, to the HI climatology generated from the NCEP–NCAR and NARR reanalyses (Winkler et al. 2007; Lu et al. 2011). The simulations for all months (not shown) indicate that the highest probability of high HI values occurs in July and August across most of the United States, with the lowest frequencies in December and January.

Focusing on the frequencies of HI $\geq$ 5 during March, August, and October (Figure 3), the percentage of days with HI $\geq$ 5 in the Western United States reaches 85 to 90 percent in August for most of the GCM-driven simulations and generally falls below 30 percent during March and October. Smaller seasonal variations are seen for the eastern and central United States, although, like the Western United States, the highest frequencies of HI $\geq$ 5 occur in July (not shown) and August.

During March and October, the frequency of HI $\geq$ 5 is larger over much of the central and eastern United States compared to the Western United States. The

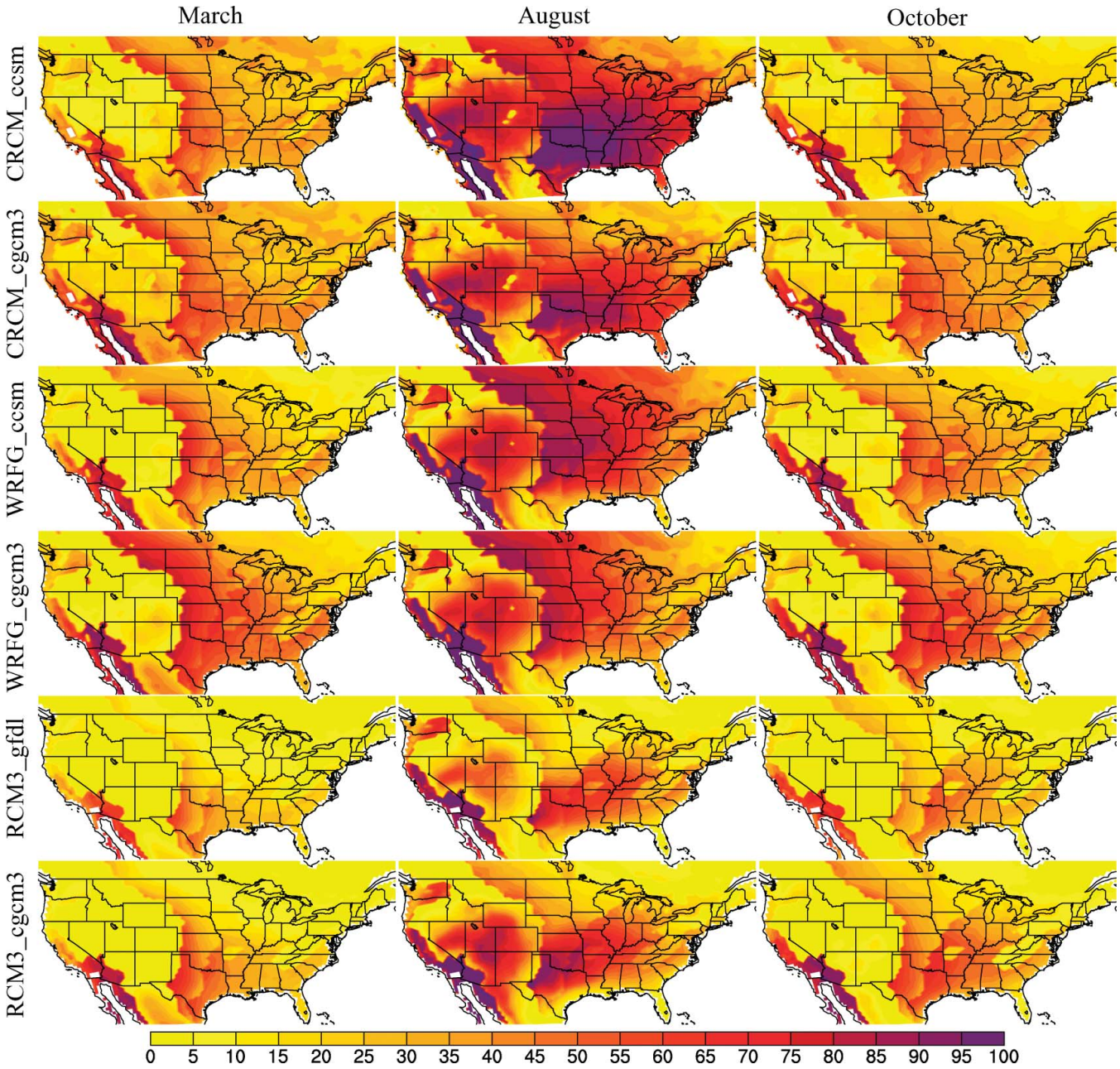

Figure 3. Percentage of days for HI $\geq$ 5 in the United States for six model combinations under current climate for March (left column), August (center column), and October (right column). (Color figure available online.)

CRCM-ccsm and CRCM-cgcm3 simulations for March and October generated similar probabilities in the central and eastern United States with peak values of nearly 50 percent over the High Plains (Figure 3). For most of the Western United States, the two CRCM runs generated probabilities ranging from 5 to 35 percent, with the CRCM-cgcm3 probabilities about 5 to 10 percent higher than those for CRCM-ccsm. The probabilities from the WRFG combinations are generally similar, although the WRFG-ccsm values are slightly lower compared to the other simulations for the Western United States, and the probabilities for the central and eastern United States from WRFG-cgcm3 are approximately 5 to 10 percent greater than those from the CRCM-cgcm3, CRCM-ccsm, and WRFG-ccsm simulations. The simulations for RCM3 have lower percentages across the domain, especially in the Midwest, compared to those for the other two RCMs. A possible reason for this difference is the much coarser vertical resolution in RCM3 (eighteen levels vs. twenty-nine in CRCM and thirty-four in WRFG), which would affect the accuracy of the lapse rate calculation as indicated by Factor A of the HI. The spatial patterns for the two RCM3 simulations also differ somewhat, with the highest values found in March in the southern Plains (Texas and Oklahoma) and in October from the southern Plains eastward along the Gulf Coast and northeastward into Arkansas and Missouri, whereas the highest values for the other RCM combinations are found in the High Plains, extending from eastern Montana to southern Texas.

During August, the two CRCM simulations and two WRFG simulations generally produced higher probabilities of HI $\geq$ 5 than the two RCM3 runs (Figure 3). Although all six model combinations display only modest differences for the central Rockies (western Colorado), southwestern United States, and the California coast, substantial between-simulation differences are observed for the eastern half of the United States. The CRCM simulations generated the highest percentages in the southern Plains and along and north of the Gulf Coast, whereas the WRFG simulations generated the highest probabilities in the central and northern Plains. The highest probabilities for the RCM3 simulations are found in northern Texas and Oklahoma, somewhat similar to the spatial pattern for the WRFG simulations, but the probabilities are much lower. Lower probabilities are also found for the RCM3 simulations over much of the Midwest and Gulf coastal region. For a particular RCM, the differences in probabilities were small between the simulations driven by different GCMs. For example, the probabilities generated by the CRCM-ccsm simulation were 5 to 10 percent higher over the central and eastern United States compared to those from the CRCM-cgcm3 simulation.

In short, for the same model run, the frequency of HI $\geq$ 5 exhibits similar spatial patterns in spring and fall, which can differ considerably from the spatial pattern in summer. The differences among model combinations are also smaller in spring and fall than in summer when large differences among model combinations are observed, especially in the High Plains and along the Gulf Coast. The probabilities are smaller for RCM3 simulations compared to those of the other model runs. Larger differences are produced when different RCMs are used for the simulations compared to when different GCMs are used.

Projected Future Changes

The simulated future HI climatology (Figure 4) for a particular RCM–GCM combination has very similar spatial patterns to the corresponding climatological pattern for the GCM-driven current climate simulation (Figure 3). The highest and lowest percentages are generally found in the same areas, suggesting that the regions currently experiencing atmospheric conditions most conducive to extreme or erratic fire behavior will likely experience those conditions in the future also. Seasonal variations are also similar for the future and current climates. To better illustrate changes in probability, the differences in the percentage of days with HI $\geq$ 5 between GCM-driven current and future climates (GCM-driven future minus GCM-driven current) were calculated for the six model combinations (Figure 5). The red (blue) shading depicts higher (lower) future probabilities of HI $\geq$ 5 compared to the current climate.

The magnitudes of the projected changes are smaller for March and October compared to August, with projected changes within $\pm$10 percent for both months. The only exception is the RCM-cgcm3 simulation, which projects a more than 20 percent increase over the central United States in October. There are considerable differences between models in the spatial patterns of the projected change, however, especially for the Great Lakes region in March and the northern and

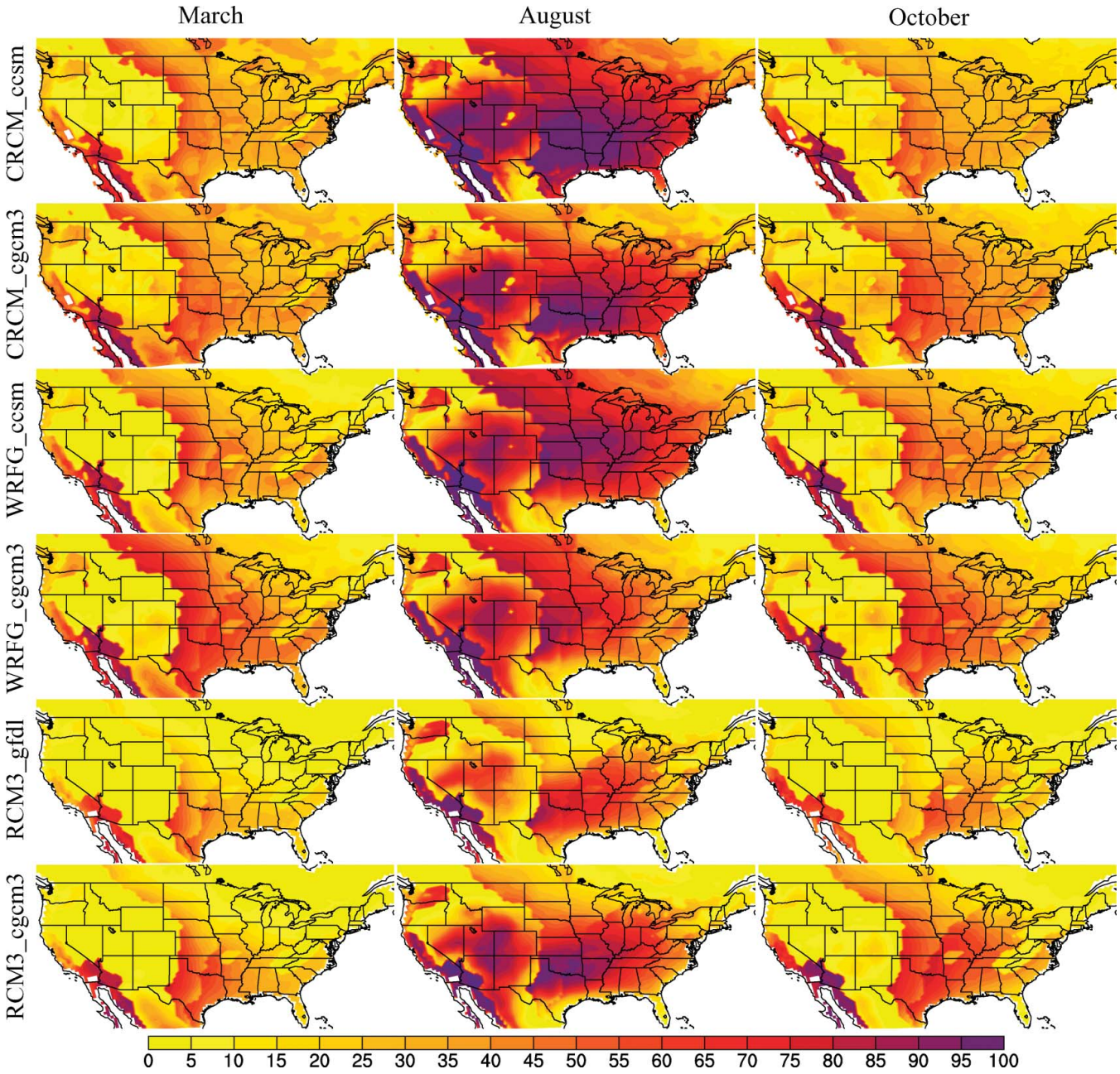

Figure 4. Percentage of days for HI $\geq$ 5 in the United States for six model combinations under future climate for March (left column), August (center column), and October (right column). (Color figure available online.)

central Plains in October, with some simulations projecting a greater future fire risk and others suggesting a smaller risk.

All of the model combinations project a higher probability of HI $\geq$ 5 during August over most of the United States under future climate conditions. The largest increases (25–35 percent) for the CRCM-ccsm and CRCM-cgcm3 simulations are found in Arizona and New Mexico. Most other areas have increases around 10 to 20 percent, although some slight decreases are observed for both simulations over parts of the northwestern United States. For the two WRFG-driven simulations, lower future probabilities are projected for the northern Plains and southern Texas, with higher risk projected elsewhere. The WRFG-ccsm simulation also suggests decreased fire risk for the Pacific Northwest, whereas lower probabilities are found in California, the Carolinas, and Georgia for the WRFG-cgcm3 simulation. Most other regions

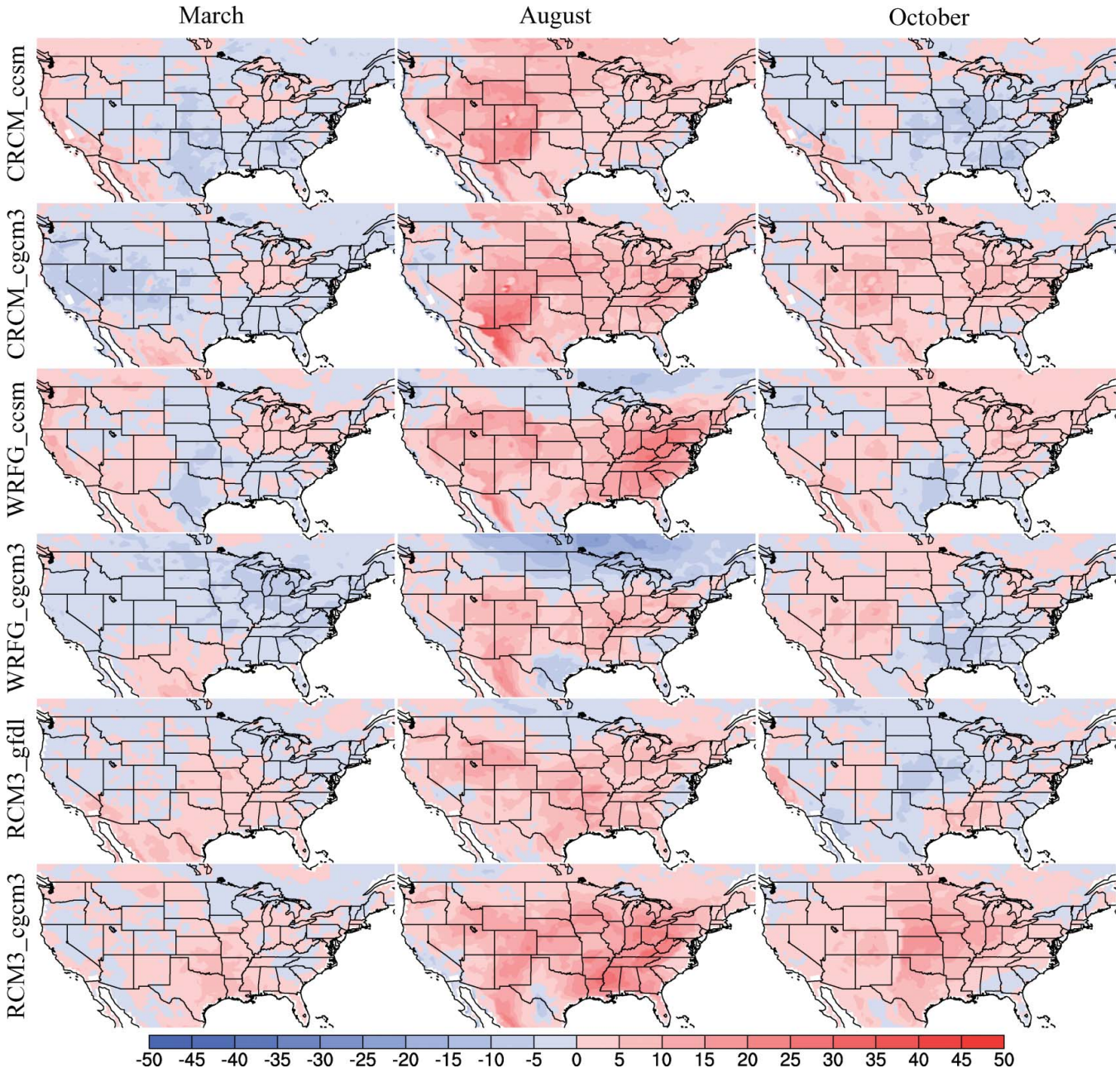

Figure 5. Change in percentage of days for HI ≥ 5 in the United States for six model combinations between current and future climate for March (left column), August (center column), and October (right column). (Color figure available online.)

exhibit increases between 10 and 25 percent. The RCM3 simulations also project increased probabilities over most of the United States, except for the northern Plains, where a decrease is simulated by the RCM3-gfdl combination.

To assess the agreement among model combinations, Figure 6 shows the standard deviation and mean values of the percentage of days with HI ≥ 5 during August for all six model combinations for the GCM-driven current and future climates and the differences between them. For both the GCM-driven current and future climates, the greatest intermodel differences in the percentage of days with HI ≥ 5 are found in the Midwest, the northern Plains, and along the Gulf Coast. The greatest disagreement in the projected future changes is found in parts of the Midwest, the Southeast, and the Southwest.

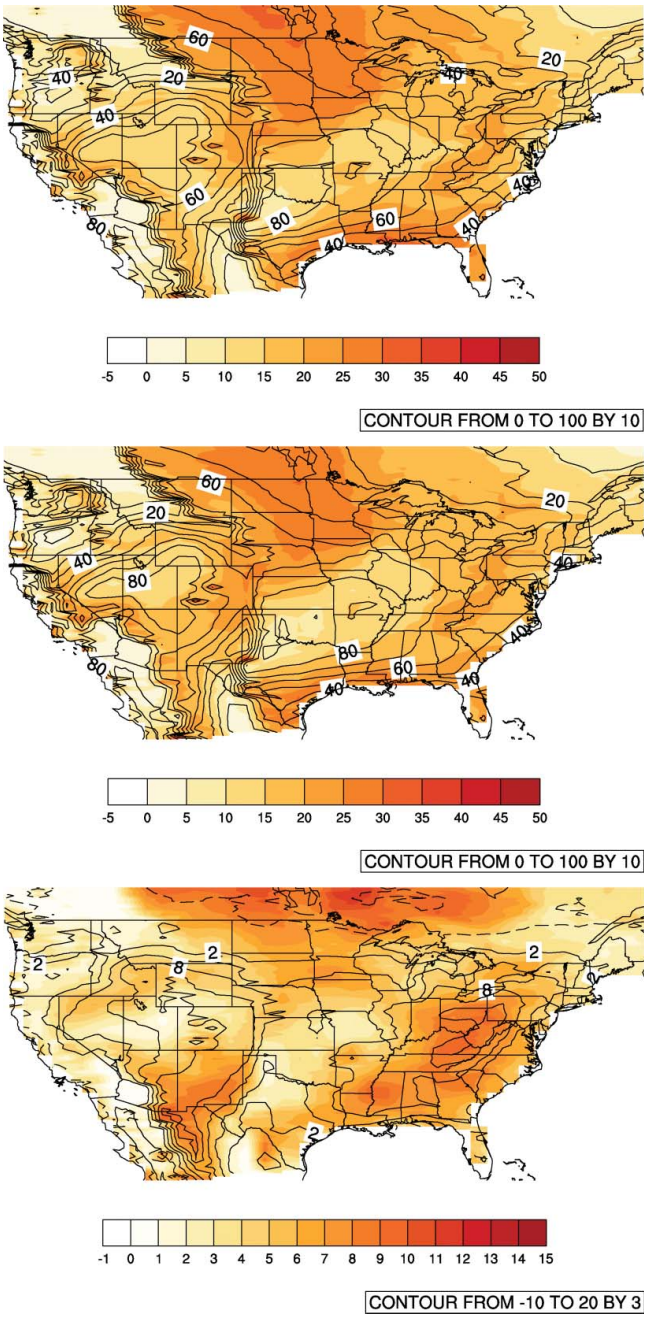

Figure 6. Mean (contour) and standard deviation (shading) of percentage of days for HI $\geq$ 5 in the United States for six model combinations for current climate (upper), future climate (center), and difference between current and future climate (lower) during August. The mean is contoured from 0 to 100 by ten intervals for current (upper) and future (center) climate and from –10 to 20 by three intervals for the change between current and future climate (lower). The standard deviation is colored from –5 to 50 by five intervals for current (upper) and future (center) climate and from –1 to 15 by one interval for the change between current and future climate (lower). (Color figure available online.)

The A and B Components

As the HI is composed of a stability factor (A) and a moisture factor (B), it is helpful to determine the relative contribution of each factor to the projected changes in the percentage of days with high HI.

Changes in the percentage of days with A = 3 between the GCM-driven current and future climate simulations are presented in Figure 7. The projected changes in the frequency of days with A = 3 for March and October are generally within ±15 percent. During March, the two RCM3 simulations show increases over most of the United States, whereas the WRFG-cgcm3 projects a large-scale decrease in frequency. The other three simulations display greater regional differences in the sign of the projected changes, with generally increased probability of A = 3 for the Great Lakes region and the Midwest and decreased frequency in the Great Plains and the Intermountain West. For October, the CRCM-cgcm3 and RCM3-cgcm3 simulations yielded increased probabilities over most of the United States, whereas the other model combinations display considerable spatial variability. For August, almost all of the model combinations project an increase in the percentage of days with A = 3 across much of the United States, with the primary exception being the Pacific coast. In addition, the WRFG-ccsm, WRFG-cgcm3, and RCM3-gfdl simulations project decreased probabilities over the north central United States.

Changes in the percentage of days with B = 3 between the GCM-driven current and future climate simulations are presented in Figure 8. The projected changes for March and October are generally within ±20 percent, although the spatial pattern of the differences varies greatly among the six model combinations. The two WRFG simulations yielded negative changes for March across much of the United States, whereas for the other simulations a projected decrease in the frequency of days with B = 3 was generally limited to New England, the northern Midwest, and the Intermountain West. During October, the CRCM-cgcm3, WRFG-cgcm3, and RCM3-cgcm3 simulations projected an increased frequency of days with B = 3 across most of the United States, whereas the other model combinations yielded more spatial variability. The general trends in the B component in August are more consistent among the different simulations compared to March and October. All of the model

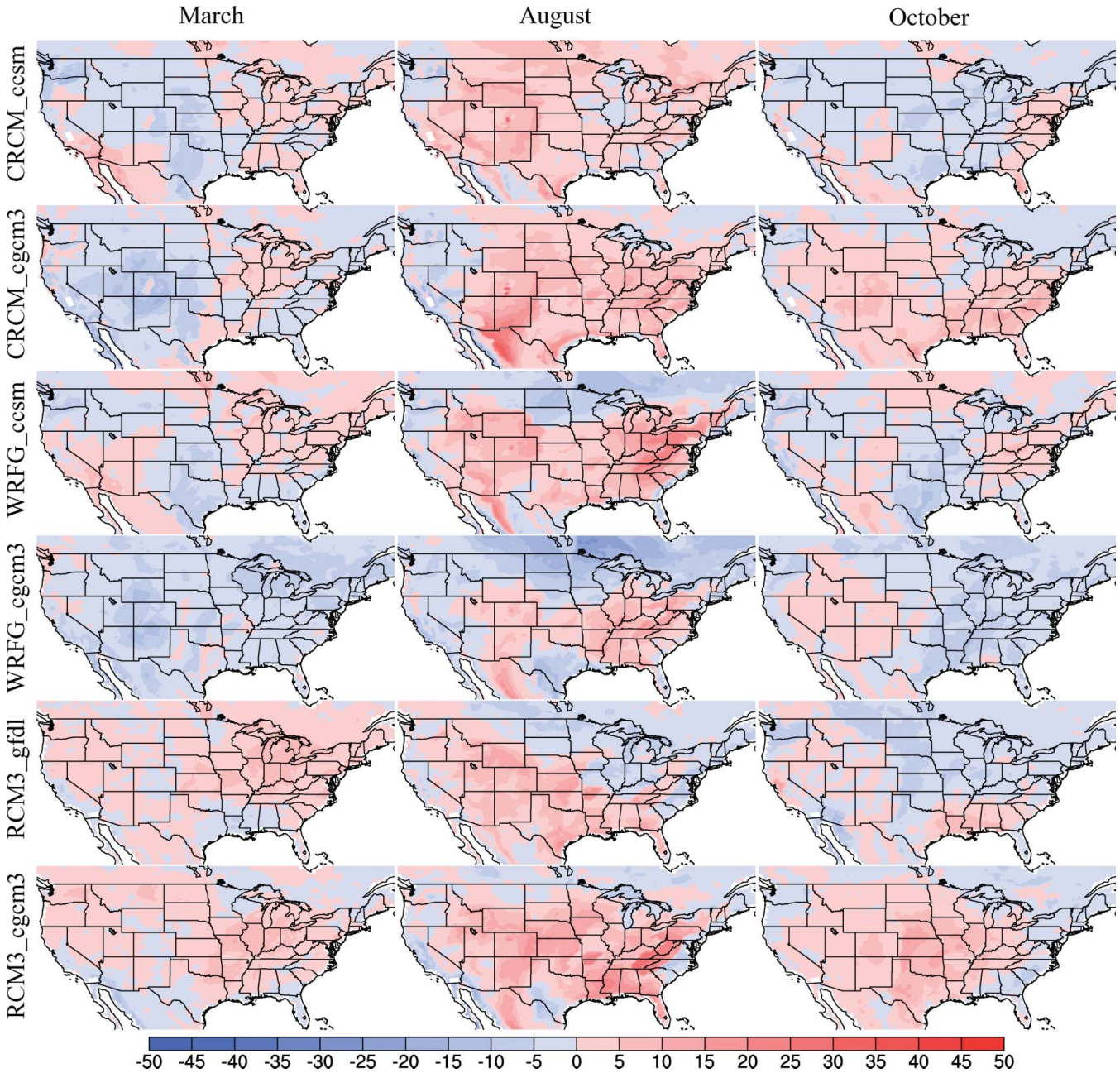

Figure 7. Change in percentage of days for A = 3 in the United States for six model combinations between current and future climate for March (left column), August (center column), and October (right column). (Color figure available online.)

combinations except for WRFG-cgcm3 project an increased frequency of days with B = 3 over most of the United States. The WRFG-ccsm simulation projects the largest positive changes (~40 percent), whereas the largest negative changes (~20 percent) are observed for the WRFG-cgcm3 simulation. These large projected changes, especially in contrast to those for the A component, suggest that the B component contributes more to the projected future increase or decrease in the probability of high HI for August.

Persistence of High HI Events

The persistence of high HI days is also an important consideration for fire management. Here, the persistence or the length of an event is determined by the

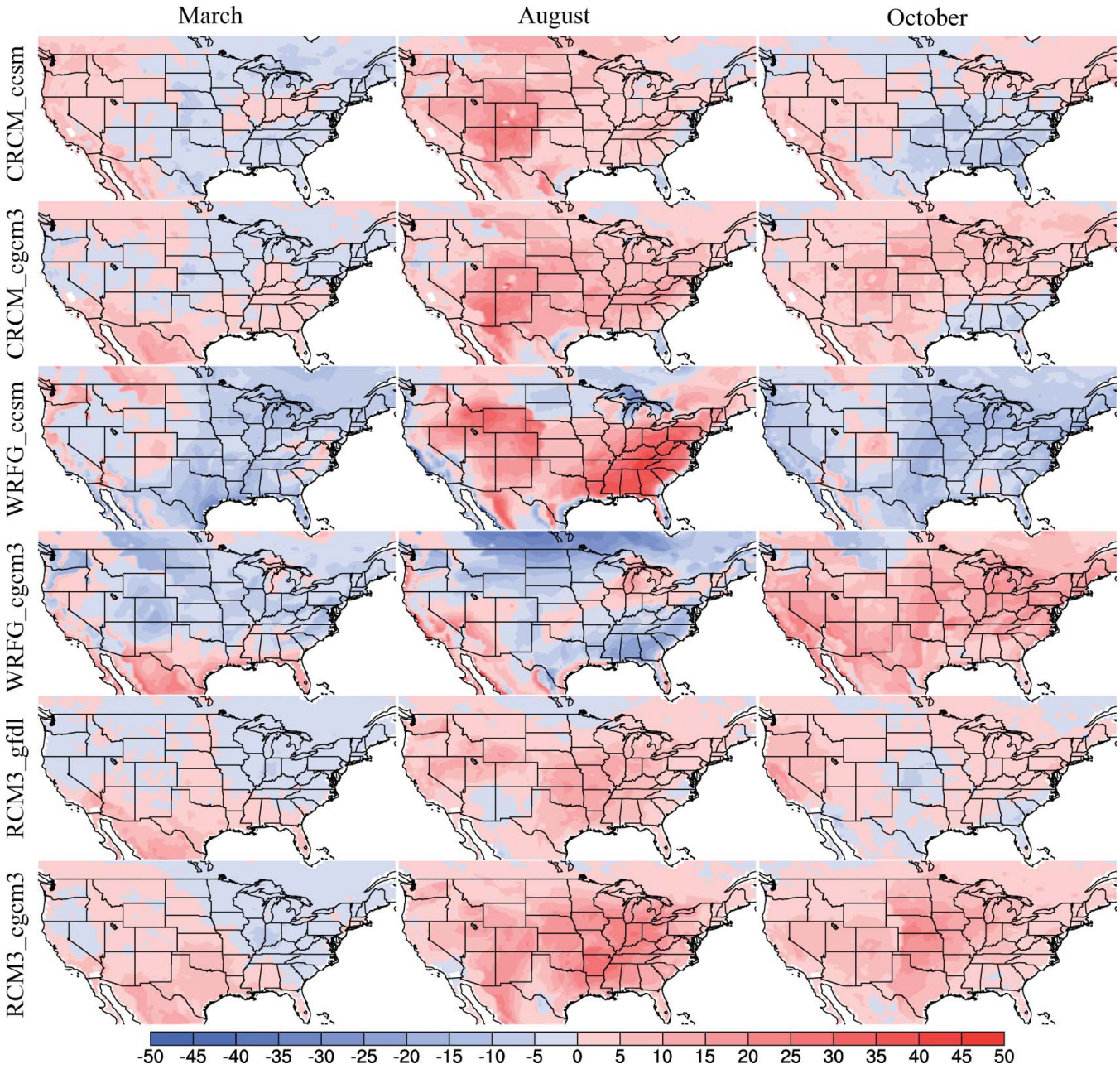

Figure 8. Change in percentage of days for B = 3 in the United States for six model combinations between current and future climate for March (left column), August (center column), and October (right column). (Color figure available online.)

number of consecutive days with HI ≥ 5. The average length of all events as well as events longer than five, thirteen, and twenty-one days is computed for the GCM-driven current and GCM-driven future climate simulations and the results are compared. The results are shown for August only to represent summer season, as prior climatological analyses (Winkler et al. 2007; Lu et al. 2011) indicate that high HI values and long events are more frequent in summer.

Projected changes in the average length of all HI ≥ 5 events in August, as generated by the GCM-driven current versus GCM-driven future climate simulations, are shown in Figure 9. The average length is projected to increase by two to five days for many regions of the United States. The two CRCM simulations and the WRFG-ccsm and RCM3-cgcm3 simulations project greater increases in the length of HI ≥ 5 events compared to the WRFG-cgcm3 and

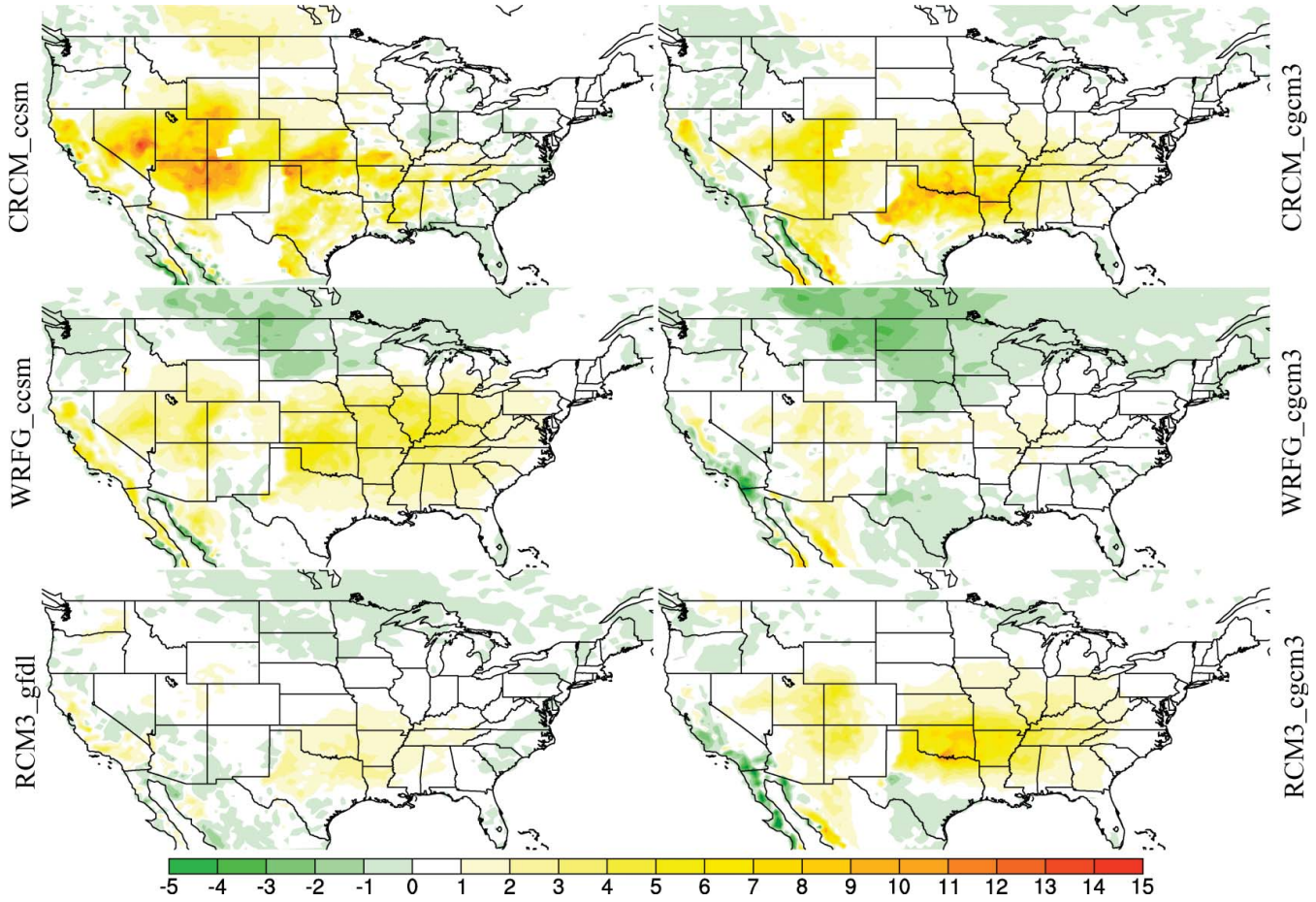

Figure 9. Change of average length of events with HI ≥ 5 for August between current and future climate. (Color figure available online.)

RCM3-gfdl simulations. The largest increases (about nine to twelve days) for the CRCM-ccsm simulation are found for the Intermountain West, whereas the CRCM-ccsm, CRCM-cgcm3, and RCM3-cgcm3 simulations project substantially longer events in Texas and Oklahoma. The two WRFG simulations and the RCM3-gfdl simulation suggest decreases in the length of HI ≥ 5 events on the order of one to three days over the northern Plains. Based on the mean and standard deviation of the future changes in HI duration (Figure 10), the models exhibit the largest discrepancies in the southern part of the Intermountain West and the southern Plains (Figure 10).

The average length of persistent high HI events that last longer than five, thirteen, and twenty-one days (events longer than one to thirty days were calculated but shown selectively) during August are presented in Figures 11 through 13, respectively. The projected changes in the average length of high HI events lasting longer than five, thirteen, or twenty-one consecutive days exhibit similar spatial patterns despite different thresholds of consecutive days (Figures 11–13). For most of the United States, the average length of these long events is projected to increase by one to four days under future climate conditions but, as can be expected, the magnitude of the increase becomes less as the threshold of consecutive days increases. For events longer than twenty-one days, many areas of United States are still projected to experience slight increases (zero to two days on average) in their frequency. These results suggest that not only could the percentage of high HI days increase in the future but the high HI events might have a longer duration. Additionally, regions with an increased number of summer days with high HI values are likely to also have longer consecutive high HI days.

Discussion

The HI was selected for this study for a number of reasons. First, this fire weather index was designed for detecting atmospheric conditions prone to extreme

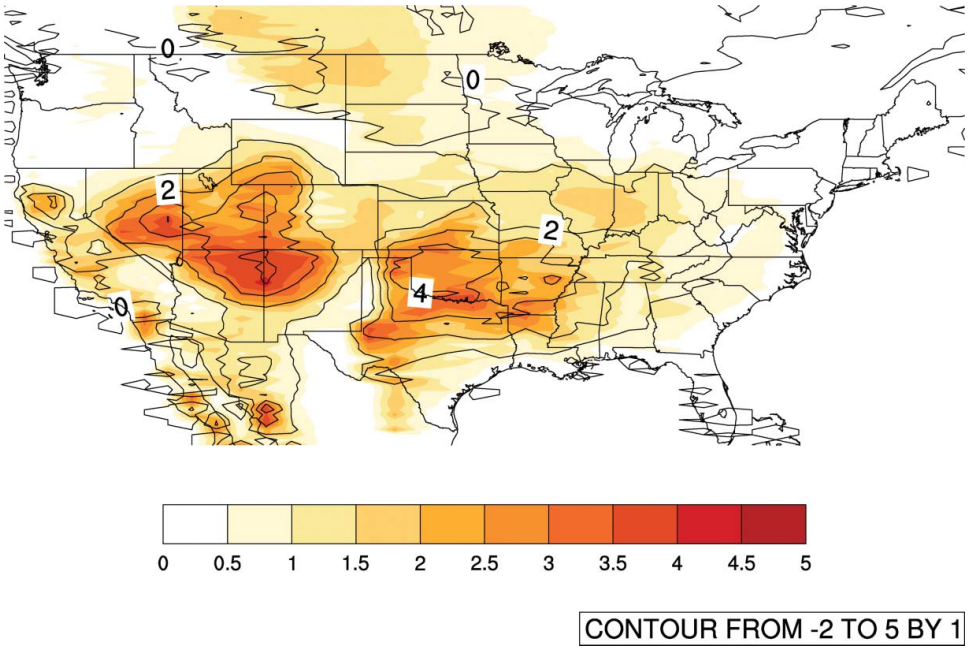

Figure 10. Mean (contour) and standard deviation (shading) of change in average length of events with HI ≥ 5 for August between current and future climate for six model combinations. The mean is contoured from –2 to 5 by 1 intervals. The standard deviation is shaded from 0 to 5 by 0.5 intervals. (Color figure available online.)

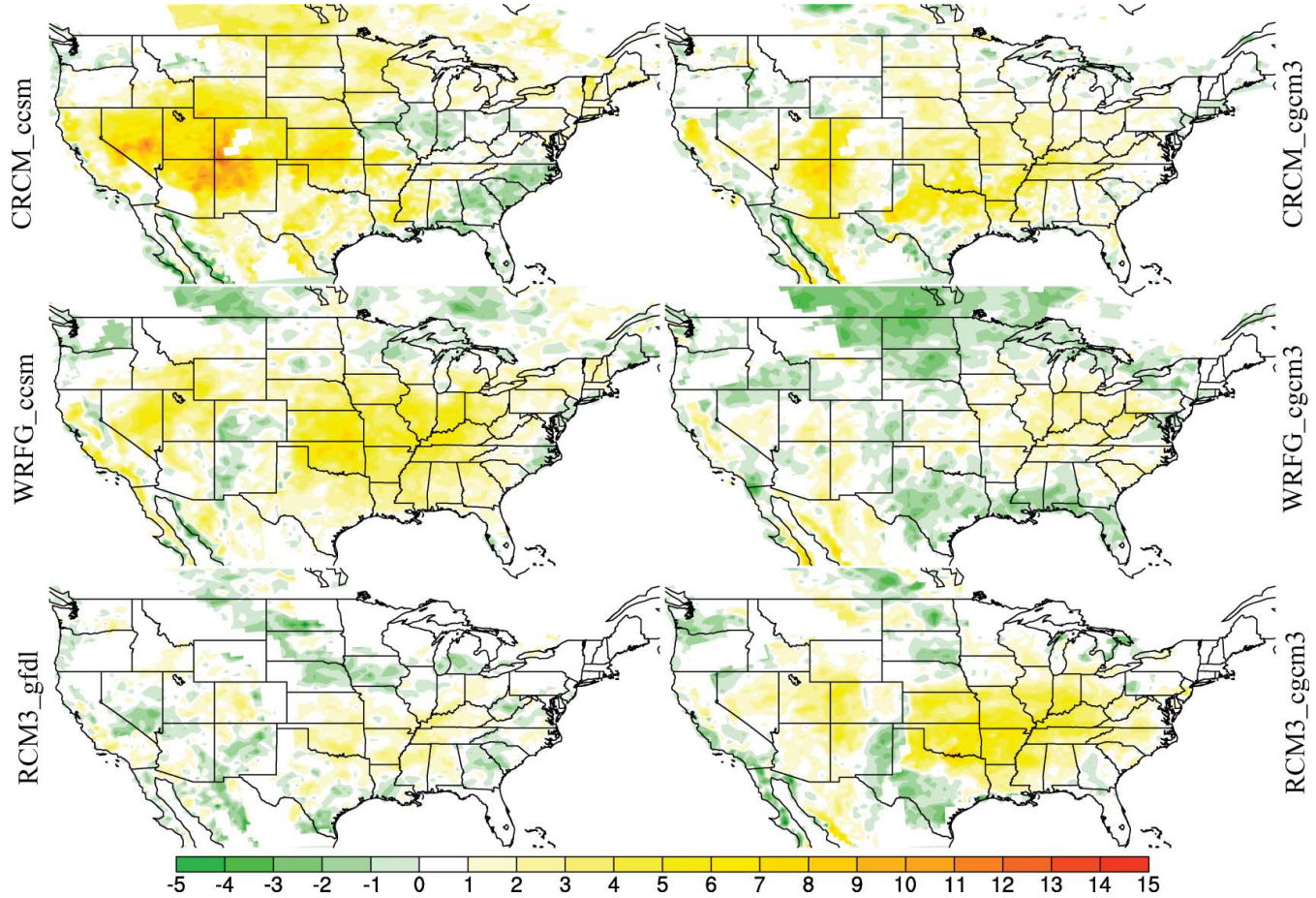

Figure 11. Change in average length of events longer than five days with HI ≥ 5 for August between current and future climate. (Color figure available online.)

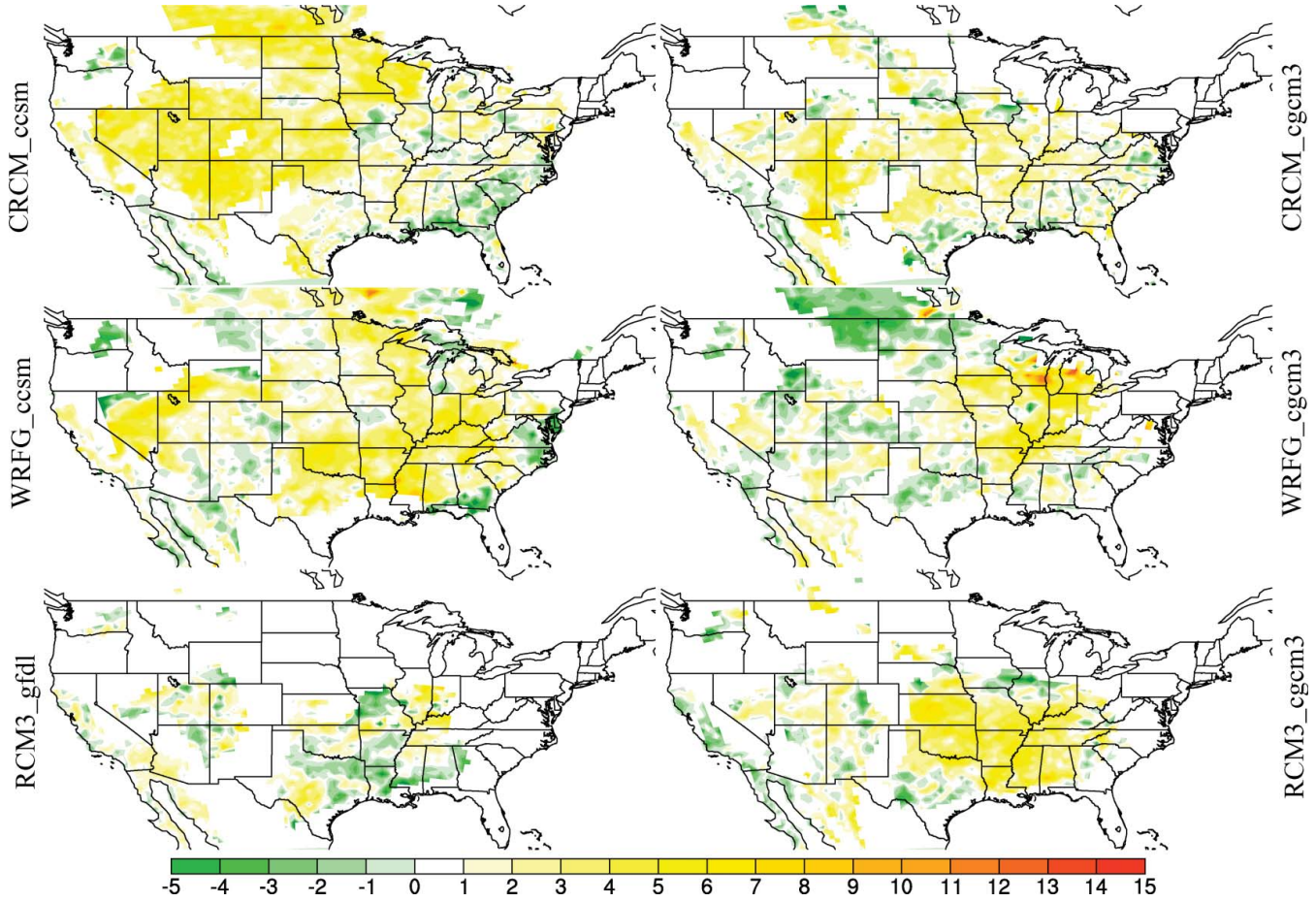

Figure 12. Change in average length of events longer than thirteen days with HI ≥ 5 for August between current and future climate. (Color figure available online.)

fire behavior. Second, HI is considered a regional-scale index because it is not sensitive to local conditions and can thus be used to provide an important perspective of the risk for wildfires to become large and erratic over a large region (Heilman and Bian 2007). Third, by considering both atmospheric stability and dryness, the HI is more informative than indexes that only consider stability or moisture alone. Finally, the HI is straightforward and convenient and has been widely used in operational fire weather forecasting. The HI also has its limitations, however. The lack of consideration of wind and turbulence in the lower atmosphere is a major limitation. The delineation of the boundaries of the low, mid, and high variants is rather subjective (Haines 1988; Winker et al. 2007), often resulting in unsmoothed transitions or discontinuities in HI values across the boundaries between the different variants. The HI can also become "saturated" in regions with typically hot, dry Mediterranean or arid climates (McCaw et al. 2007), prompting the recent proposal of a continuous HI (C-HAINES; Mills and McCaw 2010). Others (e.g., Heilman and Bian 2007) have recommended that the HI be combined with other indicators of atmospheric conditions, such as turbulent kinetic energy, to increase its effectiveness.

This study features the use of simulations from multiple combinations of RCMs driven by GCMs made available recently by NARCCAP. With their finer resolution, which allows for a better representation of factors such as topography and land cover, RCMs can describe climate feedback mechanisms acting at the regional scale (Intergovernmental Panel on Climate Change [IPCC] 2007). Previous studies concerning the impact of climate change on wildfire activity have generally employed one (Brown, Hall, and Westerling 2004) or several (Flannigan, Stokes, and Wotton 2000; Flannigan et al. 2005) coarse-resolution GCMs or a single RCM (Liu, Goodrick, and Stanturf 2013). The multimodel ensemble approach (based on six

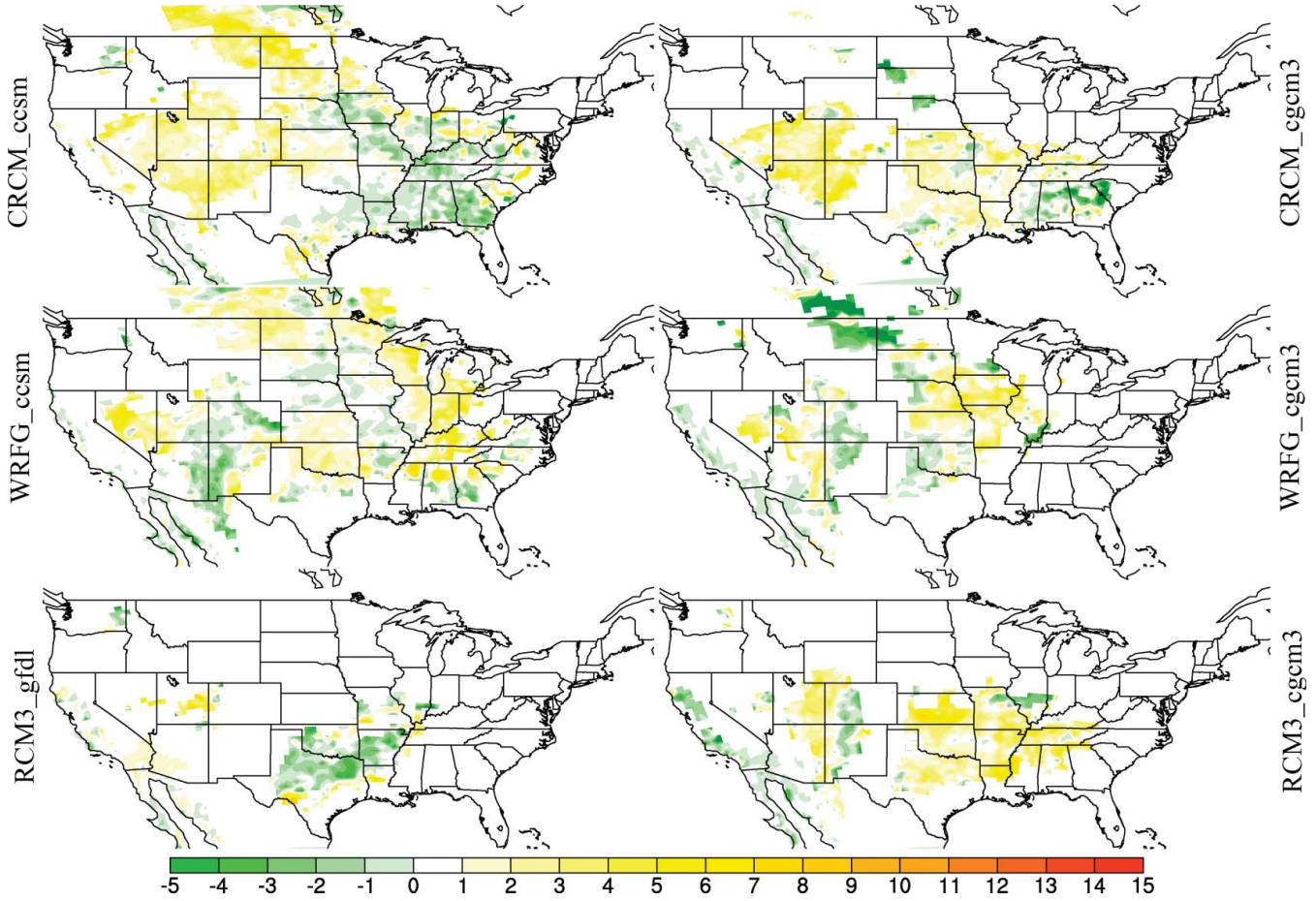

Figure 13. Change in average length of events longer than twenty-one days with HI $\geq$ 5 for August between current and future climate. (Color figure available online.)

model combinations, namely, CRCM-ccsm, CRCM-cgcm3, WRFG-ccsm, WRFG-cgcm3, RCM3-gfdl, and RCM3-cgcm3) employed in this study was adopted to increase reliability and to better depict uncertainty. Although there is considerable spatial variation in the projected changes for March and October, all model combinations consistently project an increase in the frequency of occurrence of atmospheric conditions favoring large and erratic wildfires for most of the United States in August, building more confidence into these results. One limitation, however, is that all model combinations were forced with the A2 scenario, which is on the higher end of the greenhouse gas emissions scenarios. Additional emissions scenarios should be considered in future analyses to address uncertainty in the projections arising from different emissions trajectories.

The spatial patterns of the GCM-driven HI climatology for the current climate are generally in good agreement with those of the reanalysis-derived HI climatology (Winkler et al. 2007; Lu et al. 2011). Furthermore, because the spatial patterns remain similar between the GCM-driven current and future HI climatologies, it is likely that the regions currently experiencing atmospheric conditions most conducive to extreme wildfires will also experience them in the future.

The results are generally dependent on which combination of RCM and GCM is used. Model combinations with the same RCMs for the most part produce more similar spatial patterns than model combinations with the same GCMs, implying that the differences among the model combinations are caused mainly by different RCMs rather than by different GCMs. Notwithstanding, the differences caused by GCMs can be large as well. The strong dependency of the regional projections on the specific RCM calls for extreme caution when interpreting results from a single RCM for a specific location. One direction for future study is to examine the similarities and differences among the

model combinations more closely and to validate the current climate simulations against actual fire occurrence and fire spread data to assess where a certain model or model combinations perform best. Furthermore, the mechanisms driving the change in fire potential between the current and future climate need to be studied in more detail. Another future research direction is to examine for locations where climate data are available, whether the RCM simulations improve on the estimates of future change obtained from applying statistical downscaling directly to GCM output, or whether the application of statistical downscaling to the RCM simulations would help reduce the biases in the RCM simulations.

Other factors not considered in this study, such as land-use and land-cover change (LULCC), can also directly impact fuels and thus change fire behavior. LULCC could also affect fire weather and climate by changing carbon fluxes and greenhouse gas emissions and altering atmospheric composition and radiative forcing properties (IPCC 2007). Climate modeling strategies for predicting future climate conditions typically treat land use and land cover as static or unchanging due mainly to the lack of reliable LULCC projections (Stanton et al. 2012). Given the substantial influence that LULCC can have on fuel and atmospheric conditions, models used to project future conditions for fire weather and fire behavior might need to incorporate the LULCC factor.

Conclusions

The HI serves as a straightforward and useful tool for indications of atmospheric conditions that are conducive to extreme or erratic fire behavior. In this study, the potential change in the frequency of occurrence of high HI values (and thus the potential for extreme fire behavior) and the length of consecutive days with high HI values over the contiguous United States are examined using the NARCCAP simulations. Specifically, the study employs NARCCAP simulations of the current climate and future climate from six different RCM–GCM combinations representing three RCMs (CRCM, WRFG, and RCM3) and three GCMs (CCSM, CGCM3, and GFDL). In addition, RCM runs driven by the NCEP reanalysis for the current climate are used to help identify errors introduced by the GCMs.

The spatial patterns and seasonal variations for the percentage of days with HI $\geq$ 5 across the United States for the six model combinations are found to be very similar between the current and future climate conditions, suggesting that the regions that are currently experiencing higher potential for large and erratic wildfires due to favorable atmospheric conditions alone would continue to do so in the future. Despite GCM biases, the simulation results suggest that most regions of the United States might see an increase in the percentage of days with HI $\geq$ 5 during the summer season by midcentury. The simulations also suggest that the average duration of HI $\geq$ 5 episodes in the summer might be longer under future climate conditions compared to current climate conditions for most of the United States. Further analysis indicates that the moisture component of the HI contributes more to the projected changes than the stability component. Several key regions (Intermountain West, High Plains, and Gulf Coast region) with high potential for large and erratic fires in the future were identified, and this information could be used by fire and land managers for the purpose of long-term planning and designing strategies for climate change adaptation. Discrepancies occur among the projections from the six model combinations for spring and fall, which limits confidence in future changes for these seasons. The results also show that the HI climatology patterns from simulations using the same RCM are more similar than those using the same GCM. The projected future changes need to be interpreted in terms of the limitations of the HI and with respect to the limitations of the regional and global climate models.

References

Bradshaw, L. S., J. E. Deeming, R. E. Burgan, and J. D. Cohen. 1984. The 1978 National Fire Danger Rating system: Technical documentation. General Technical Report INT-169, U.S. Department of Agriculture, Forest Service, Intermountain Forest and Range Experiment Station, Ogden, UT.

Brown, T., B. Hall, and A. Westerling. 2004. The impact of twenty-first century climate change on wildland fire danger in the Western United States: An applications perspective. *Climatic Change* 62:365–88.

Caya, D., and R. Laprise. 1999. A semi-implicit semi-Lagrangian regional climate model: The Canadian RCM. *Monthly Weather Review* 127:341–62.

Collins, W. D., C. M. Bitz, M. L. Blackmon, G. B. Bonan, C. S. Bretherton, J. A. Carton, P. Chang, et al. 2006. The Community Climate System Model: CCSM3. *Journal of Climate* 19:2122–43.

Croft, P. J., M. Watts, and B. E. Potter. 2001. The analysis of the Haines Index climatology for the eastern United States, Alaska, Hawaii, and Puerto Rico. In *Fourth Symposium on Fire and Forest Meteorology*, Paper No. 8.7. Boston: American Meteorological Society. http://ams.confex.com/ams/4FIRE/techprogram/programexpanded_83.htm

Dayananda, P. W. A. 1977. Stochastic models for forest fires. *Ecological Modelling* 3:309–13.

Deeming, J. E., R. E. Burgan, and J. D. Cohen. 1977. The National Fire-Danger Rating System. General Technical Report INT-39, U.S. Department of Agriculture, Forest Service, Intermountain Forest and Range Experiment Station, Ogden, UT.

Delworth, T. L., A. J. Broccoli, A. Rosati, R. J. Stouffer, V. Balaji, J. A. Beesley, W.F. Cooke et al. 2006. GFDL's CM2 global coupled climate models. Part I: Formulation and simulation characteristics. *Journal of Climate* 19:643–74.

Flannigan, M. D., M. A. Krawchuk, W. J. de Groot, B. M. Wotton, and L. M. Gowman. 2009. Implications of changing climate for global wildland fire. *International Journal of Wildland Fire* 18:483–507.

Flannigan, M. D., K. A. Logan, B. D. Amiro, W. R. Skinner, and B. J. Stocks. 2005. Future area burned in Canada. *Climate Change* 72:1–16.

Flannigan, M. D., B. J. Stokes, and B. M. Wotton. 2000. Forest fires and climate change. *The Science of the Total Environment* 262:221–29.

Flato, G. M. 2005. The third generation coupled global climate model (CGCM3). http://www.ec.gc.ca/ccmac-cccma/default.asp?n=1299529F-1 (last accessed 29 October 2013).

Giorgi, F. 2006. Regional climate modeling: Status and perspectives. *Journal de Physique IV France* 139: 101–18.

Golding, N., and R. Betts. 2008. Fire risk in Amazonia due to climate change in the HadCM3 climate model: Potential interactions with deforestation. *Global Biogeochemical Cycles* 22:GB4007.

Gordon, C., C. Cooper, C. A. Senior, H. Banks, J. M. Gregory, T. C. Johns, J. F. B. Mitchell, and R. A. Wood. 2000. The simulation of SST, sea ice extents and ocean heat transports in a version of the Hadley Centre coupled model without flux adjustments. *Climate Dynamics* 16:147–68.

Grell, G. A., and D. Devenyi. 2002. A generalized approach to parameterizing convection combining ensemble and data assimilation techniques. *Geophysical Research Letters* 29:1693–97.

Haines, D. 1988. A lower atmosphere severity index for wildlife fires. *Fire Weather* 13:23–27.

Heilman, W. E., and X. Bian. 2007. Combining turbulent kinetic energy and Haines Index predictions for fire-weather assessments. In *Proceedings of the Fire Environment-Innovations Management and Policy*, ed. B. W. Butler and W. Cook, 159–72. Fort Collins, CO: U.S. Department of Agriculture Forest Service Rocky Mountain Research Station.

Intergovernmental Panel on Climate Change (IPCC). 2007. *Climate change 2007*. Cambridge, UK: Cambridge University Press.

Jones, K. M., and C. Maxwell. 1998. A seasonal Haines Index climatology for New Mexico and the significance of its diurnal variations in the elevated Southwest. In *Preprints of the Second Symposium on Fire and Forest Meteorology*, 127–30. Phoenix, AZ: American Meteorological Society.

Keetch, J. J., and G. Byram. 1968. A drought index for forest fire control. Research Paper SE-38, U.S. Department of Agriculture, Forest Service, Southeastern Forest Experiment Station, Asheville, NC.

Knapp, E. E., B. L. Estes, and C. N. Skinner. 2009. Ecological effects of prescribed fire season: A literature review and synthesis for managers. General Technical Report No. PSW-GTR-224, U.S. Department of Agriculture, Forest Service, Pacific Southwest Research Station, Albany, CA.

Kochtubajda, B., M. D. Flannigan, J. R. Gyakum, and R. E. Stewart. 2001. The influence of atmospheric instability on fire behavior in the Northwest Territories, Canada. In *Fourth Symposium on Fire and Forest Meteorology*, 225–232. Reno, NV: American Meteorological Society.

Laprise, R., D. Caya, M. Giguère, G. Bergeron, H. Côté, J.-P. Blanchet, G. J. Boer, and N. McFarlane. 1998. Climate and climate change in western Canada as simulated by the Canadian Regional Climate Model. *Atmosphere-Ocean* 36:119–67.

Liu, Y., S. L. Goodrick, and J. A. Stanturf. 2013. Future U.S. wildfire potential trends projected using a dynamically downscaled climate change scenario. *Forest Ecology and Management* 294:120–35.

Liu, Y., J. A. Stanturf, and S. L. Goodrick. 2010. Trends in global wildfire potential in a changing climate. *Forest Ecology and Management* 259:685–97.

Lu, W., J. Charney, S. Zhong, X. Bian, and S. Liu. 2011. A North American regional reanalysis climatology of the Haines Index. *International Journal of Wildland Fire* 20: 91–103.

Luo, L., Y. Tang, S. Zhong, X. Bian, and W. E. Heilman. 2013. Will future climate favor more erratic wildfires in the Western United States? *Journal of Applied Meteorology Climatology* 52:2410–17.

Mandallaz, D., and R. Ye. 1997. Prediction of forest fires with Poisson models. *Canadian Journal of Forest Research* 27:1685–94.

McCaw, L., P. Marchetti, G. Elliott, and G. Reader. 2007. Bushfire weather climatology of the Haines Index in southwestern Australia. *Australian Meteorological Magazine* 56:75–80.

Mearns, L. O., R. Arritt, S. Biner, M. Bukovsky, S. Sain, D. Caya, D. Flory, et al. 2012. The North American Regional Climate Change Assessment Program: Overview of Phase I results. *Bulletin of the American Meteorological Society* 93:1337–62.

Mearns, L. O., W. J. Gutowski, R. Jones, L. Leung, S. McGinnis, A. M. B. Nunes, and Y. Qian. 2009. A regional climate change assessment program for North America. *EOS* 90:311–12.

Mearns, L., S. McGinnis, R. Arritt, S. Biner, P. Duffy, W. Gutowski, I. Held, et al. 2007. *The North American Regional Climate Change Assessment Program dataset*. Boulder, CO: National Center for Atmospheric Research Earth System Grid. https://www.earthsystemgrid.org/project/NARCCAP.html (last accessed 19 October 2014).

Mills, G. A., and L. McCaw. 2010. *Atmospheric stability environments and fire weather in Australia: Extending the Haines Index*. CAWCR Technical Report 20, Centre for Australian Weather and Climate Research, Melbourne, Australia.

Nakicenovic, N., J. Alcamo, G. Davis, H. J. M. de Vries, J. Fenhann, S. Gaffin, K. Gregory, et al. 2000. *Special report on emissions scenarios: A special report of Working Group III of the Intergovernmental Panel on Climate Change*. Cambridge, UK: Cambridge University Press.

National Interagency Fire Center. 2013. Total wildland fires and acres (1960–2012). http://www.nifc.gov/fireInfo/fireInfo_stats_totalFires.html (last accessed 29 October 2013).

National Oceanic and Atmospheric Administration. 2014. Terms commonly used in fire weather forecast. http://www.erh.noaa.gov/okx/glossary.html (last accessed 18 February 2014).

Pal, J. S., F. Giorgi, X. Bi, N. Elguindi, F. Solmon, S. A. Rauscher, X. Gao, et al. 2007. The ICTP RegCM3 and RegCNET: Regional climate modeling for the developing world. *Bulletin of the American Meteorological Society* 88:1395–1409.

Parisien, M. A., V. Kafka, N. Flynn, K. G. Hirsch, J. B. Todd, and M. D. Flannigan. 2005. Fire behavior potential in central Saskatchewan under predicted climate change. PARC Summary Document 05-01, Prairie Adaptation Research Collaborative, Regina, Canada.

Pielke, R. A., W. R. Cotton, R. L. Walko, C. J. Tremback, W. A. Lyons, L. D. Grasso, M. E. Nicholls, M. D. Moran, D. A. Wesley, T. J. Lee, and J. H. Copeland. 1992. A comprehensive meteorological modeling system—RAMS. *Meteorology and Atmospheric Physics* 49: 69–91.

Pitman, A. J., G. T. Narisma, and J. McAneney. 2007. The impact of climate change on the risk of forest and grassland fires in Australia. *Climate Change* 84:383–401.

Preisler, H. K., D. R. Brillinger, R. E. Burgan, and J. W. Benoit. 2004. Probability based models for estimating wildfire risk. *International Journal of Wildland Fire* 13: 133–42.

Preisler, H. K., and A. L. Westerling. 2007. Statistical model for forecasting monthly large wildfire events in Western United States. *Journal of Applied Meteorology and Climatology* 46:1020–30.

Schmidt, G. A., R. Ruedy, J. E. Hansen, I. Aleinov, N. Bell, M. Bauer, S. Bauer, et al. 2006. Present day atmospheric simulations using GISS ModelE: Comparison to in-situ, satellite and reanalysis data. *Journal of Climate* 19:153–92.

Skamarock, W. C., J. B. Klemp, J. Dudhia, D. O. Gill, D. M. Barker, W. Wang, and J. G. Powers. 2005. A description of the Advanced Research WRF Version 2. NCAR Tech Notes 468+STR, National Center for Atmospheric Research, Boulder, CO.

Spracklen, D. V., L. J. Mickey, J. A. Logan, R. C. Hudman, R. Yevich, M. D. Flannigan, and A. L. Westerling. 2009. Impacts of climate change from 2000 to 2050 on wildfire activity and carbonaceous aerosol concentrations in the Western United States. *Journal of Geophysical Research* 114:D20301.

Stanton, J. C., R. G. Pearson, N. Horning, P. Ersts, and H. Reşit Akçakaya. 2012. Combining static and dynamic variables in species distribution models under climate change. *Methods in Ecology and Evolution* 3:349–57.

Werth, J., and P. Werth. 1998. Haines index climatology for the Western United States. *Fire Management Notes* 58: 8–17.

Westerling, A., A. Gershunov, T. Brown, D. Cayan, and M. Dettinger. 2003. Climate and wildfire in the Western United States. *Bulletin of the American Meteorological Society* 84:595–604.

Williams, J. T. 2004. Managing fire-dependent ecosystems: We need a public lands policy debate. *Fire Management Today* 64:6–11.

Winkler, J. A., R. W. Arritt, and S. C. Pryor. 2014. Climate projections for the Midwest: Availability, interpretation, and synthesis. In *Climate change in the Midwest: A synthesis report for the National Climate Assessment*, ed. J. A. Winkler, J. A. Andresen, J. Hatfield, D. Bidwell, and D. Brown, 37–63. Washington, DC: Island.

Winkler, J. A., G. S. Guentchev, M. Liszewska, Perdinan, and P. Tan. 2011. Climate scenario development and applications for local/regional climate change impact assessments: An overview for the non-climate scientist. *Geography Compass* 5: 301–28.

Winkler, J. A., B. E. Potter, D. F. Wilhelm, R. P. Shadbolt, K. Piromsopa, and X. Bian. 2007. Climatological and statistical characteristics of the Haines Index for North America. *International Journal of Wildland Fire* 16: 139–52.

Correspondence: Department of Geography, Michigan State University, East Lansing, MI 48824; e-mail: tangying@msu.edu (Tang); zhongs@msu.edu (Zhong); lluo@msu.edu (Luo); winkler@msu.edu (Winkler). U.S. Department of Agriculture Forest Service, Lansing, MI 48910; e-mail: xbian@fs.fed.us (Bian); wheilman@fs.fed.us (Heilman).